

# ON THE TOPOLOGICAL STRUCTURE OF THE QCD VACUUM

*Problems and Results of Lattice Studies*

ION-OLIMPIU STAMATESCU

*ITP, U. Heidelberg, Philosophenweg 16, D-69120 Heidelberg*

AND

*FEST, Schmeilweg 5, D-69118 Heidelberg, Germany*

**Abstract:** A review of results from lattice studies using improved and scale controlled cooling methods is presented and their significance is discussed. The improvement of the action ensures stable instanton solutions of physical sizes. The scale controlled cooling can be generally used as a gauge invariant low pass filter to extract the physics from noisy MC configurations; in particular it preserves instanton-antiinstanton pairs selected according to their interaction. We apply these methods to analyze various features of the topological structure of the Yang-Mills vacuum in a scaling invariant way.

## 1. Introduction

This article presents results from a series of works involving besides the above author the following persons in various combinations:

PH. DE FORCRAND (ETH Zürich and TH-Div., CERN, Switzerland),

M. GARCÍA PÉREZ (Dept. Fís. Teor., Univ. Aut. de Madrid, Spain),

T. HASHIMOTO (Dept. of Appl. Physics, Fukui Univ., Japan),

J.E. HETRICK (Physics Dept., U. of the Pacific, Stockton, USA),

S. HIOKI (Dept. of Physics, Tezukayama Univ., Nara, Japan),

E. LAERMANN (FB Physik, Univ. Bielefeld, Germany),

J.F. LAGAE (HEP Div., Argonne Nat. Lab., USA),

H. MATSUFURU (RCNP, Osaka, Japan),

O. MIYAMURA, T. UMEDA (Dept. of Physics, Hiroshima Univ., Japan),

A. NAKAMURA (RIISE, Hiroshima Univ., Japan),

O. PHILIPSEN (Th. Div., CERN, Genève, Switzerland),

T. TAKAISHI (Hiroshima University of Economics, Japan).

The simulations and results on which the following discussions are based are described in [1],[2],[3],[4],[5],[6],[7].

## 2. Physical Questions and Problems of the Analysis

Instantons are self-dual solutions of the Euclidean field equations mapping the  $SU(2)$  color group space on the 3-d sphere at spatial infinity (for  $SU(N_c)$  the  $SU(2)$  subgroups are relevant). They are defined among other by winding number (topological charge) and position and size parameters. The  $\mathbf{R}^4$  (anti-)instanton (A)I has charge (q) and action (s) densities [8]:

$$q(x) = \frac{1}{8\pi^2} F^* F = \frac{6Q}{\pi^2 \rho^4} \left[ 1 + \sum_{\mu=1}^4 \left( \frac{x_\mu - x_\mu^0}{\rho} \right)^2 \right]^{-4}, \quad s(x) = S_0 |q(x)|, \quad (1)$$

$$Q = \int d^4 x q(x) = \pm \text{integer}, \quad S = \int d^4 x s(x) = |Q| S_0, \quad S_0 = 8\pi^2.$$

In  $\mathbf{T}^4$  only  $|Q| \neq 1$  exist [9]. In  $\mathbf{R}^3\mathbf{T}$  (relevant at non-zero temperature  $T$ ) the “caloron” [10] describes objects flattening in the Euclidean time direction and of limited spatial size  $\rho \leq \sqrt{3}/\pi T$ . Finally, various kinds of twisted boundary conditions allow for new solutions [11],[12]. Superpositions of  $N$  I’s or A’s also correspond to (higher) minima of the action:  $S = NS_0$ . A pair I-A is not, however, a minimum and  $S^{IA}$  depends also on “overlap”  $\omega$ :

$$S^{IA} = 2S_0 - S_{\text{int}}^{IA} < 2S_0, \quad \omega = (\rho_I + \rho_A)/d_{IA}, \quad d_{IA} = |x_I^0 - x_A^0|. \quad (2)$$

Effects associated with instantons are (for a review see [13]):

- the  $U_A(1)$  symmetry breaking (via the Witten - Veneziano formula[14]),
- chiral symmetry breaking (via zero modes of the Dirac operator),
- dynamical effects for the physics at intermediate distances.

The first one only involves global topological properties (susceptibility). The other possible effects depend on details of the local structure, like density and size distribution of instantons, and the calculation involves models. In the *instanton liquid model* [15], for instance, which is the standard model of instanton physics, various predictions have been made [13]. Numerical simulations should test the ingredients used in these models. Thereby:

- The instantons can be in a gas, liquid, or crystalline phase. The diluteness is expressed by the “packing fraction”

$$f = \frac{\pi^2 \langle \rho^4 \rangle N}{2V}. \quad (3)$$

- The size distribution controls diluteness and I-R properties. There is no prediction for large sizes. For small sizes the dilute gas approximation gives:

$$P(\rho) \sim \rho^p, \quad p_{\text{dilute}} = -5 + b, \quad b = 11N_c/3 \quad (4)$$

- Denoting by  $N_I(N_A)$  the number of I's (A's) in a configuration, and with  $N = N_I + N_A$ ,  $Q = N_I - N_A$  we write:

$$c_P \equiv (\langle N^2 \rangle - \langle N \rangle^2) / \langle N \rangle. \quad (5)$$

For a poissonian distribution  $c_P = 1$ , while low energy sum rules suggest  $c_P = \frac{4}{b}$  [16]. A further measure for the character of the I,A distribution is:

$$c_{\text{int}} = \frac{\langle N_I N_A \rangle - \langle N_I \rangle \langle N_A \rangle}{\sqrt{(\langle N_I^2 \rangle - \langle N_I \rangle^2)(\langle N_A^2 \rangle - \langle N_A \rangle^2)}} = \frac{\langle N^2 \rangle - \langle Q^2 \rangle - \langle N \rangle^2}{\langle N^2 \rangle + \langle Q^2 \rangle - \langle N \rangle^2} \quad (6)$$

which tests the correlation between I's and A's:  $c_{\text{int}}$  is 0 if there is no such correlation, but goes to 1 if I and A appear correlated (e.g., pairwise).

For non-perturbative analysis one resorts to lattice simulations. The Monte Carlo method is sometimes considered to be a tool which produces numerical results, without improving our understanding of the physical mechanisms. This view, however, has turned out to be too narrow and different structural questions have been investigated by means of Monte Carlo calculations. The problems such an analysis of the topological structure encounters are twofold. *Problems of principle* are:

- UV-divergences in correlation functions like  $\langle q(x)q(0) \rangle$  which contain the susceptibility information in a contact term (notice that  $\langle q(x)q(0) \rangle < 0$  for disjoint supports, e.g. for  $x \geq 2a$  if  $F_{\mu\nu}$  is defined on plaquettes) [17].

- Dislocations: concentration of topological charge on one or few plaquettes. They have action smaller than  $S_0$  and may be produced copiously, spoiling the measurement of  $Q$  and the continuum limit [18].

- Since  $S_{\text{int}}^{\text{IA}} < 2S_0$  close pairs can be easily produced. With increasing overlap it becomes difficult to define genuine I-A pairs as distinguished from short range density fluctuations and the description in terms of I's and A's becomes questionable [3].

It appears therefore that a certain amount of smoothing may be necessary to define topology on the lattice. *Practical problems* are:

- The need to develop smoothing methods which can be controlled in a physical way. They should be based on independent physical arguments, leave the investigated structure undistorted and allow to observe its properties without making assumptions about them. In particular scaling behaviour of topological distributions should not be assumed but revealed.

- The description of the topological structure in terms of I's and A's. Overlapping structures, especially with opposite charges, become difficult to fit with a superposition ansatz based on (1). One needs to introduce various criteria and some measure for the adequacy of the description which, however, remains imperfect.

### 3. Scale Controlled Cooling [5],[6]

The problem of developing good smoothing methods has been approached in a number of ways: standard cooling, smearing, blocking, combination of them and others [19],[20],[21],[22]. The smoothing is controlled by monitoring, by giving a blocking step or by tuning smearing to approximate a RG transformation with fixed point action etc. The most natural control for a smoothing method, however, is by giving the smoothing radius or wave length threshold and we should like, therefore, to develop a method systematically controlled by a physical scale. We start from cooling, since this procedure is analytically defined (by reference to the equations of motion) and has as fixed point nontrivial semi-classically relevant configurations with  $N = |Q|$ . Cooling, which proceeds by local minimization of a given lattice action, works as a diffusion process, smoothing out increasingly large regions [23]. Thereby properties of the physical spectrum measured from correlations at a given distance are affected, in particular the string tension drops rapidly with the number of cooling sweeps  $n_c$  [24]. Instantons may be distorted and lost during cooling by bad scaling properties of the action and also by I-A annihilation. The susceptibility may be spoiled by dislocations. We thus need:

- 1) To use an action with practically scale invariant instanton solutions and a sharp dislocation threshold *fixed in lattice units* to eliminate UV noise (dislocations) while shrinking in approaching continuum, and
- 2) To ensure that cooling is controlled by a physical smoothing scale such that the structure at larger scales remains unchanged. Monitoring and engineering should not be necessary, since this may introduce arbitrariness.

The *Restricted Improved Cooling* (RIC) introduced in [5] fulfills these requirements. RIC acts as a *gauge invariant low pass filter* preserving physics at scales above a *cooling radius*  $r_c$  which can be fixed unequivocally, while smoothing out the structure below  $r_c$ . In particular the string tension is preserved beyond  $r_c$ , instantons are stable, dislocations are eliminated, and I-A pairs are retained above an overlap threshold depending on  $r_c$ .

RIC uses the action of the *Improved Cooling* algorithm (IC) with 5 planar, fundamental Wilson loops [25],[1]. This action is correct to order  $\mathcal{O}(a^6)$  and has a *dislocation threshold*  $\rho_0/a = \hat{\rho}_0 \sim 2.3$ , below which short range topological structure is smoothed out (note that  $\rho_0 \rightarrow 0$  in approaching continuum). Above  $\rho_0$ , instantons are stable under IC to any degree of cooling (however, I-A pairs annihilate). The corresponding *improved charge density* using the same combination of loops leads to an integer charge already after a few cooling sweeps and stable thereafter. See Fig. 1.

Recall that the cooling algorithm is derived from the equations of motion

$$U_\mu(x)W_\mu(x)^\dagger - W_\mu(x)U_\mu(x)^\dagger = 0, \quad (7)$$

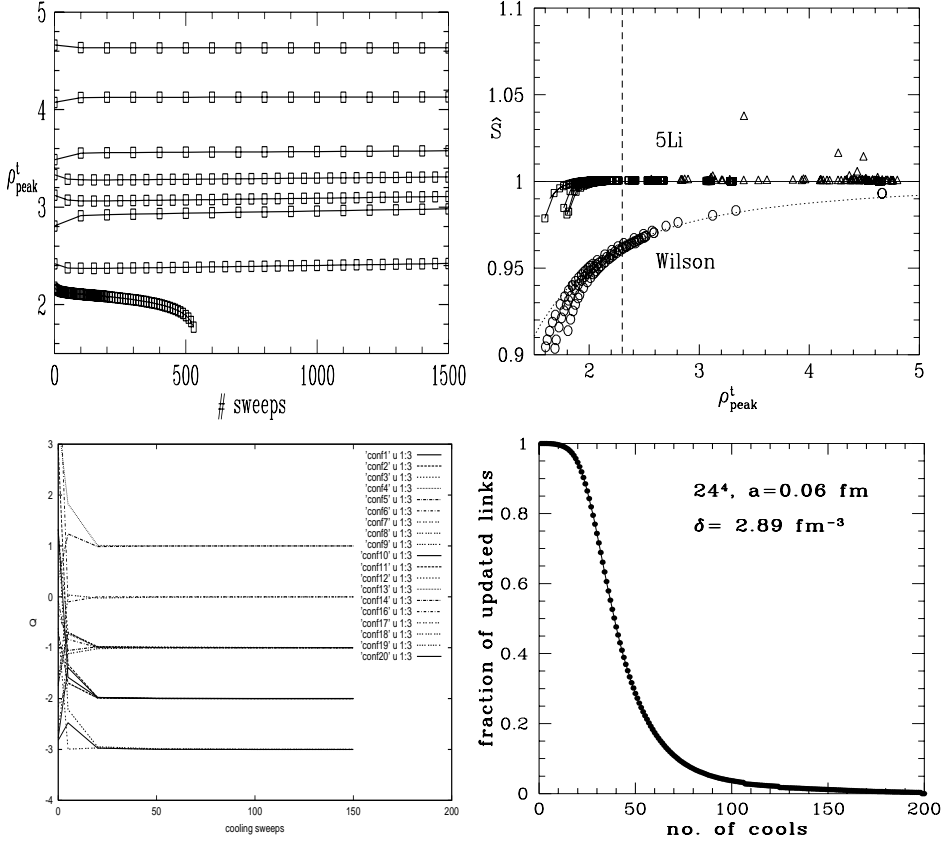


Figure 1. IC and RIC properties: Evolution of sizes of single instantons (upper left). Improved (5Li) and Wilson action *vs* instanton size given in lattice units;  $\rho_{peak}$  is defined in [1] (upper right). Evolution of the improved charge  $Q$  for 20  $SU(3)$  MC configurations [7] (lower left). Saturation of cooling for RIC: fraction of updated links as function of the cooling sweeps – for stopped standard cooling or IC this would be a step function (lower right).

where  $W$  is the sum of staples connected to the link  $U_\mu(x)$  in the action, as (we restrict here to  $SU(2)$ , for the general case see [5]):

$$U \rightarrow U' = V = W/||W||, \quad ||W||^2 = \frac{1}{2}\text{Tr}(WW^\dagger). \quad (8)$$

We define RIC by the constraint that only those links be updated, which violate the equation of motion by more than some chosen threshold<sup>1</sup>:

$$U \rightarrow V \quad \text{iff} \quad \Delta_\mu(x)^2 = a^{-6}\text{Tr}(1 - UV^\dagger) \geq \delta^2. \quad (9)$$

<sup>1</sup>We thank F. Niedermayer for this suggestion.

We have  $\Delta_\mu^2(x) \propto -\text{Tr}((D_\nu F_{\nu\mu}(x))^2)$  in continuum limit [26]. Thus  $\delta$  controls the energy of the fluctuations around classical solutions and acts as a filter for short wavelengths. Since it uses the same action RIC has the same scaling properties as IC. However, since RIC does not update links already close to a solution, it changes fewer links after every iteration until the algorithm saturates – see Fig. 1. (9) defines a constrained minimization and the smoothing is homogeneous over the lattice (see [5]).

Since the parameter  $\delta$  which defines the cooling is already a physical quantity it should be related to a physical scale. For Yang Mills theory the latter involves the string tension  $\sigma$ . We calculate the “effective mass”  $M(t)$  from correlation functions of spatial Polyakov loops separated by  $t$  steps in time. Asymptotically  $M(t) \simeq N_s \sigma$  up to finite size corrections.

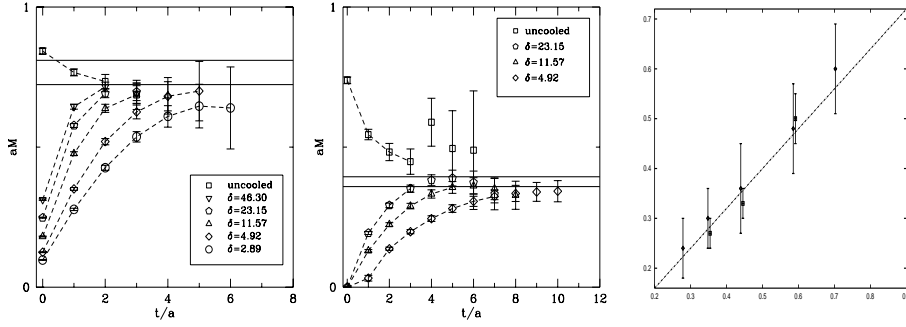


Figure 2. Left and middle:  $M(t)$  for the  $a = 0.12$  (0.06) fm lattice [5]. Horizontal bands represent standard results for  $\sigma$ . Right: The smoothing scale of RIC  $r_c(\delta)$  vs  $\delta^{-1/3}$  for the  $a = 0.12$  fm (diamonds) and  $a = 0.06$  fm (squares) lattices. Also shown is the fit (10).

We present in Fig. 2  $M(t)$  for  $SU(2)$ . Defining  $r_c(\delta)$  as the distance  $t$  at which  $M(t)$  on  $\delta$ -cooled configurations starts to agree with the uncooled value (obtained by fuzzing and fitted to a smooth function of  $t$ ) we arrive at the results in Fig. 2 (right) showing the scaling behaviour expected from the continuum limit of the parameter  $\delta$ , compatible with

$$r_c(\delta) \simeq 0.8 \delta^{-1/3}. \quad (10)$$

The behaviour of instantons is similar under RIC and IC. RIC has a dislocation threshold depending on  $a^3\delta$ ,  $\rho_0(a^3\delta) = \hat{\rho}_0(a^3\delta)a$  approaching the IC dislocation threshold from below:  $\hat{\rho}_0(a^3\delta) \leq \hat{\rho}_0(0) \equiv \hat{\rho}_0 = 2.3$ . Fixing  $\delta$  and rescaling  $\beta$  to approach the continuum limit the RIC threshold shrinks similarly to the IC one. Instantons above the dislocation threshold are preserved unchanged both by RIC (independently on  $r_c$ ) and by IC (independently on cooling sweeps), since both algorithms use the same action

with scale invariant instanton solutions. I-A pairs, however, do not annihilate under RIC the way they do for the other cooling methods (including IC): since the distortion of the partners in a pair depends on the overlap, RIC preserves pairs below some overlap-threshold. More precisely, there is a well defined relation between  $\Delta_\mu$  (measured at the center of the partners or at mid-distance between them) and  $S_{\text{int}}^{\text{IA}}$  eq. (2). Thus RIC stabilizes I-A pairs with  $S_{\text{int}}^{\text{IA}}$  below a threshold depending on  $r_c(\delta)$ .

#### 4. Topological Properties of Yang-Mills Theories at $T = 0$

##### 4.1. GLOBAL PROPERTIES [1],[3],[5],[6]

The topological charge given by IC is already after a few cooling sweeps an integer to about 1% and stable thereafter. Similarly,  $Q$  given by RIC is also an integer and independent on  $\delta$  if the cooling radius is larger than the dislocation threshold,  $r_c > \rho_0 \sim 2a$ . The topological charge distribution is therefore well defined. It also agrees excellently, e. g., with the distribution obtained by using overlap fermions [27]. The topological susceptibility obtained in this way is well defined, shows good scaling properties and agrees with the Witten-Veneziano relation. See Table 1.

	$SU(2)$	$SU(2)$	$SU(3)$	$SU(3)$	$QCD$	$QCD$	$QCD$
Latt.	$12^3 36$	$24^4$	$12^4$	$16^4$	$24^3 12$	$24^3 12$	$24^3 12$
bound. cond.	pbc	tbc	tbc	tbc	apbc	apbc	apbc
$a$ (fm)	0.12	0.06	0.134	0.1	0.115	0.103	0.0855
$\chi^{1/4}$ (MeV)	195(4)	200(8)	184(6)	182(7)	134(10)	102(5)	0

TABLE 1.  $\chi^{1/4}$  for pure Yang-Mills at  $T = 0$  [1],[3],[5] (average) and for QCD at  $T \simeq 0.85, 0.98$  and  $1.13T_c$  [3]. The results are given for  $n_c > 20$  or  $r_c > 2a$ .

##### 4.2. LOCAL PROPERTIES [1],[3],[5],[6],[7]

###### 4.2.1. Description of the I-A Ensemble and Overview of the Results

In extracting the instanton information out of the configurations we approximate the action and charge density by a superposition of self-dual, non-interacting I's and A's parameterized through the 1-instanton BPST ansatz (1) (partially corrected for periodicity by adding images). We measure the departure of the real action and charge density from the above

non-interacting ansatz through the quantities

$$\varepsilon_s = \sqrt{\frac{\int d^4x |s(x) - s_{\text{fit}}(x)|^2}{\int d^4x |s(x)|^2}}, \quad \varepsilon_q = \sqrt{\frac{\int d^4x |q(x) - q_{\text{fit}}(x)|^2}{\int d^4x |q(x)|^2}}. \quad (11)$$

In the actual proceeding every time an instanton candidate is located, it is counted only if, by adding it to  $s_{\text{fit}}$  and  $q_{\text{fit}}$ ,  $\varepsilon_{s,q}$  simultaneously decrease. Of course this description misses more complicated topological structures (e.g., fractional charge) – it is a question of self-consistency to apply it within a picture of the instanton ensemble consisting of typical, self-dual I's and A's in weakly interacting superpositions. Attempts to use a more general description have been made in the literature [28], their theoretical understanding appears to us difficult, however.

This analysis is performed at a given degree of smoothness and we ask about the stability of the results with the latter. Our attitude is that significant dependency on the smoothing degree can reflect, may be unwanted, but real properties of the instanton ensemble. To judge about this scaling tests are essential. Normal cooling and even IC reveal the smoothing dependence as dependence on the number of cooling steps. The latter, however, has only an indirect physical meaning [23]. It needs to be calibrated in some way with  $\beta$  (see [1],[31] and for a recent systematic attempt [32]), the criterion for the calibration remaining, however, just the property which one wants to prove, namely scaling. RIC, on the other hand, has an automatic, natural calibration via the physical (dimensionfull) cooling scale  $r_c$ . The cooling is independent on  $\beta$  if  $r_c$  is larger than the shrinking dislocation threshold  $\rho_0$ , and therefore provides a genuine scaling check [5]. We then consider any  $r_c$  dependence which subsists the scaling test as potentially relevant and do not attempt a further treatment of the data (e.g., extrapolation to 0 smoothing degree [22],[29]) since we are not clear about the physical basis of the dependence and of the treatment.

An overview of the  $T = 0$  RIC and IC  $SU(2)$  results is given in Table 2, for  $SU(3)$  and  $QCD$  we refer to [3].

#### 4.2.2. Instanton Size Distributions

As can be seen from Fig. 3 the size distributions show remarkable stability under changing the RIC smoothing scale and under rescaling of the lattice spacing, up to a limited variation of the position of the maximum (notice that these are normalized distributions, the number of instantons varies by more than a factor 5 between small and large  $r_c$ ). Also the IC data show the same stability, both for  $SU(2)$  and for  $SU(3)$  – see Fig. 3. The distributions are little (at larger  $a$ ) or not affected (at smaller  $a$ ) by the dislocation threshold. The average sizes  $\rho_{av}$  are  $0.4 \pm 0.04$  fm for  $SU(2)$  and  $0.55 \pm 0.06$  fm for  $SU(3)$ , with full widths of about 0.2 (0.25) fm, respectively.



a	$\delta$	$r_c(\delta)$	$\langle N/V \rangle$	$\langle  Q  \rangle$	$\langle d_{II} \rangle$	$\langle d_{IA} \rangle$	$\varepsilon_q (\varepsilon_s)$	$\langle \rho \rangle$
0.12	23.15	0.30(5)	14.86(7)	2.8(1)	0.39	0.28	0.75(0.55)	0.38
"	11.57	0.35(5)	8.72(2)	2.93(9)	0.46	0.36	0.60(0.45)	0.40
"	4.92	0.48(5)	4.21(2)	2.91(6)	0.54	0.49	0.45(0.35)	0.42
"	2.89	0.60(5)	2.70(3)	2.85(8)	0.59	0.58	0.35(0.30)	0.44
"	IC(20)		2.06(2)	2.91(8)	0.61	0.61	0.30(0.30)	0.42
0.06	23.15	0.27(3)	18.7(1)	1.7(1)	0.40	0.30	0.60(0.45)	0.35
"	11.57	0.33(3)	9.6(1)	1.7(1)	0.48	0.39	0.45(0.40)	0.38
"	4.92	0.50(3)	4.35(6)	1.8(1)	0.57	0.53	0.25(0.25)	0.40
"	IC(50)		2.96(5)	1.7(1)	0.59	0.57	0.25(0.25)	0.37

TABLE 2.  $SU(2)$  results for IC at 20 and 50 cooling sweeps and for RIC at various  $\delta$  [5] – see also Table 1. The lattice spacing ( $a$ ), the cooling radius ( $r_c(\delta)$ ), distances and sizes are given in fm. The density  $\langle N/V \rangle$  is in  $\text{fm}^{-4}$  and  $\delta$  in  $\text{fm}^{-3}$ . The errors are statistical only, when they are not explicitly quoted they amount to about 1 in the last indicated digit.

Since the variation of  $\rho_{av}$ , which may have different origins [30], is rather limited we are tempted to consider this quantity as well defined (inside errors accounting for the various uncertainties) – see also Fig. 5. The small size branch of the distribution grows more slowly than the power law of the dense gas approximation (a fit gives  $p = 1.2 \pm 0.5$  for  $SU(2)$  and  $p = 2.5 \pm 1.0$  for  $SU(3)$ , instead of  $p_{\text{dilute}} = 2.33$  and  $p_{\text{dilute}} = 6$ , respectively) which indicates that in the region of small but relevant sizes the dilute gas picture is not adequate. The large size behaviour of the distributions cannot be determined from these simulations since instantons of size significantly above  $1/3$  of the lattice can show finite lattice size effects and already  $\rho_{av}$  is near this point (0.48 fm for  $SU(2)$  and 0.53 fm for  $SU(3)$ ; but the existence and position of the maximum are safe from this point of view).

#### 4.2.3. Instanton Density and Pair Properties

The number  $N$  of I's and A's observed at small cooling radius is essentially due to pairs ( $|Q|$  is constant and relatively small) – see Table 2. We notice that while  $N$  increases by roughly a factor 5 when  $r_c$  is decreased from about 0.6 fm to about 0.25 fm,  $\rho_{av}$  only varies by about 10%. Consequently, the packing fraction  $f$  (3) also increases approaching 1, which indicates that at small  $r_c$  we observe a rather dense ensemble, strongly

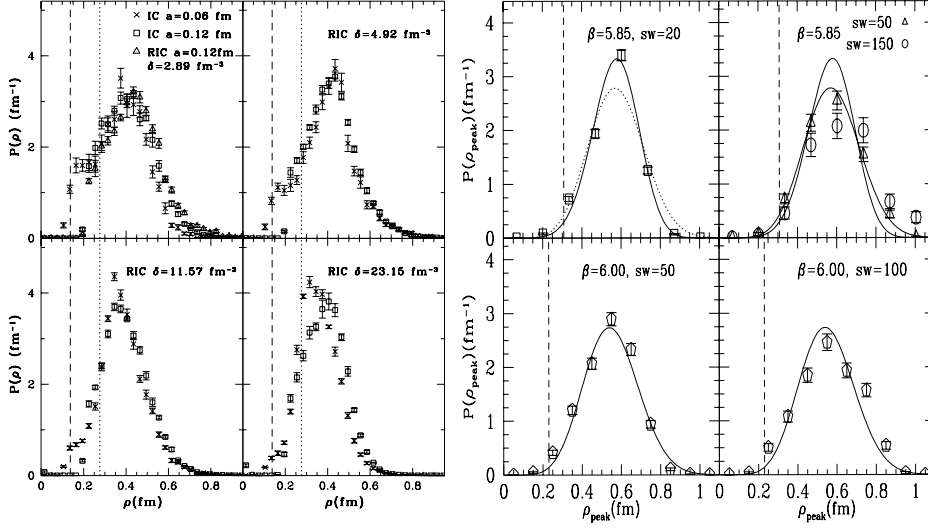


Figure 3. Left: Normalized size distributions for  $SU(2)$  from RIC and IC on the  $12^3 36$ , pbc,  $a = 0.12$  fm lattice (squares, triangles) and on the  $24^4$ , tbc,  $a = 0.06$  fm lattice (crosses) [5]. The RIC data correspond to  $r_c \sim 0.56, 0.47, 0.35$  and  $0.28$  fm ( $\delta = 2.89, 4.92, 11.57$  and  $23.15 \text{ fm}^{-3}$ , respectively). Vertical dotted (dashed) lines indicate the IC dislocation threshold  $\rho_0 = 2.3a$  for  $a = 0.12$  ( $0.06$ ) fm. The corresponding RIC dislocation thresholds are lower. Right: Normalized size distributions for  $SU(3)$  from IC on the  $12^4$ , tbc,  $a = 0.134$  fm lattice (squares, circles, triangles) and on the  $16^4$ , tbc,  $a = 0.1$  fm lattice (octagons) [3]. The curves are Gaussian fits, the dashed lines  $\rho_0 = 2.3a$ .

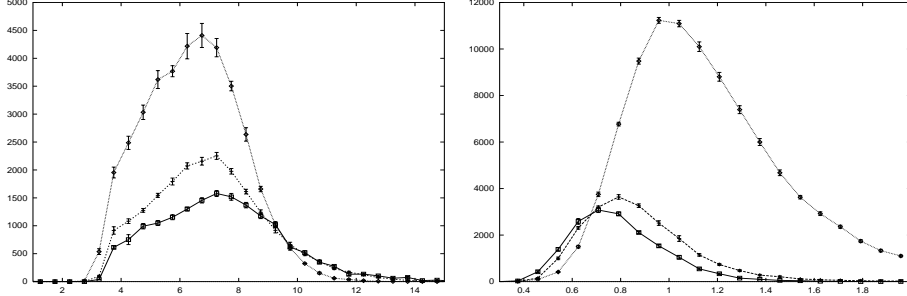


Figure 4. Non-normalized size and overlap distributions from RIC at  $a = 0.12$  fm [5] for smoothing scales  $r_c \sim 0.56$  (squares),  $\sim 0.47$  (pluses) and  $\sim 0.28$  (diamonds) fm. The scale for sizes is  $0.06$  fm.

deviating from Poisson distribution (cp eq. (5) is about 0.5) and with a tendency to charge neutralization in small regions (see [1],[31]). The overlap (2) distribution shifts toward larger values [6] while the average average distance of an I to the nearest A ( $d_{IA}$ ) decreases. See Fig. 4. The situation is succinctly described in Fig. 5. Here we plot  $SU(2)$  RIC data for averages from two lattices ( $a = 0.12$  fm and  $a = 0.06$  fm) at given  $r_c = 0.8\delta^{-1/3}$ ,

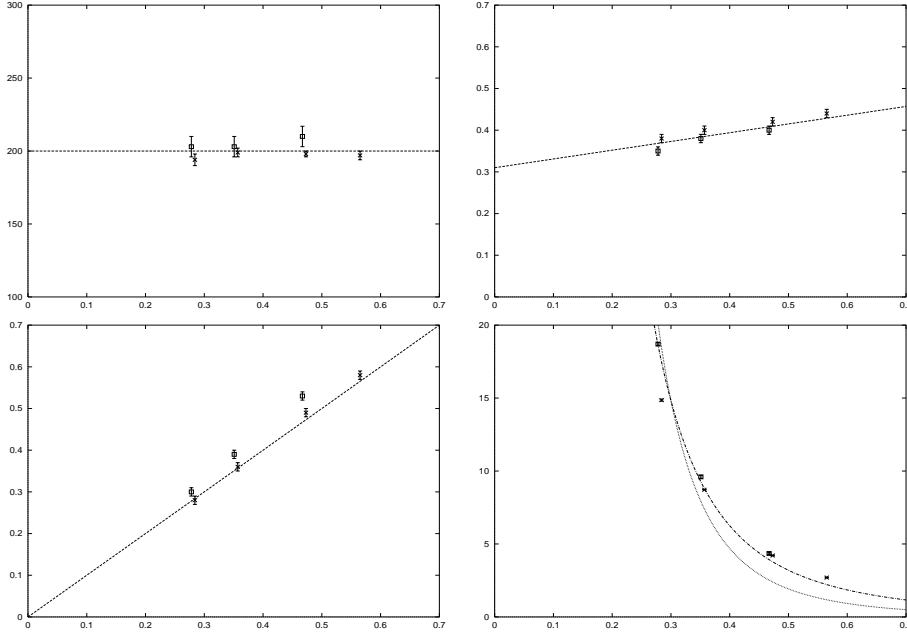


Figure 5. Smoothing scale dependence of:  $\chi^{1/4}$  (upper left), average I(A) size (upper right), average I-A distance, (lower left) and average density (lower right) for  $SU(2)$  at  $a = 0.12$  fm (crosses) and  $a = 0.06$  fm (squares) [5].  $r_c$  is taken from the fit (10), the horizontal errors (not shown) are about 0.04 fm – see also Table 2. The lines illustrate linear (dashed),  $r_c^{-3}$  (dashed-dotted) or  $r_c^{-4}$  (dotted) behaviour.

see eq. (10), i.e., the dimensionless  $\delta a^{-3}$  is simply rescaled with  $a$  at fixed  $\delta$ . As already noticed, we see that the susceptibility  $\chi$  and the average size  $\rho_{av}$  scale well with the cut-off and show no ( $\chi$ ) or little dependence ( $\rho_{av}$ ) on the smoothing scale. Also the average I-A distance and the density of I(A)’s have comparable values on the two lattices and seem therefore to scale. However, their dependence on  $r_c$  is disturbing: the instanton density increases as an inverse power of  $r_c$  and the average I-A distance is practically given by  $r_c$  itself. Simultaneously with increasing density also the quality of the fit decreases ( $\varepsilon_q$ ,  $\varepsilon_s$  increase, see Table 2). This suggests that the structure revealed at small smoothing scale (large frequencies) is strongly overlapping and distorted. Generally it appears that a “typical” density or I-A distance could only be defined by first fixing the smoothing scale. By contrast, the average size seems to have a well defined meaning for itself. Finally, restricting smoothing to scales below 0.25 fm retains too much short range fluctuations. We stress that the cut-off rescaling of these results is done without any ad-hoc fit of cooling parameters.<sup>2</sup>

<sup>2</sup>The small, systematic difference of a few percents between the “ $a = 0.12$  fm” and the “ $a = 0.06$  fm” data for all observables (including  $\sigma$  and  $\chi$ ) [5] may be due to a minimal uncertainty in assessing the value of  $a$  [1] as taken from the literature.

## 5. Topology at $T > 0$ and the Chiral Connection [2],[3],[4],[7]

A first impression on the connection between topology and chiral properties (see [33] for a recent review) is obtained at  $T = 0$ , e. g., by using the definition of the topological charge via the Ward identities for Wilson fermions [34] or via the overlap formalism [27] and comparing with the improved topological charge measured by IC or RIC. In Fig. 6, left plot, we present the topological charge distribution measured on a  $12^4$ ,  $SU(2)$  lattice ( $a = 0.12$  fm, pbc [1]) by IC and by overlap formalism [27]. See also [35].

Increasing the temperature above  $T_c$  produces radical changes in the topological properties: the susceptibility drops and the instanton ensemble seems to change its character [36],[3],[2]. Above  $T_c$  practically all configurations are in the  $Q = 0$  sector although at small  $r_c$  RIC reveals a quite large  $N$  (a similar thing is observed with IC at small number of cooling sweeps). The ensemble consists of nearby opposite charges, but it is difficult to say if these form “molecules” or just a strongly fluctuating background. The description in terms of I’s and A’ becomes difficult (the fit deteriorates). On Fig. 6, right plot, we show the I-A correlation parameter  $c_{\text{int}}$  (6) for the full QCD, MILC configurations below and above  $T_c$  [37].

It is interesting to observe the correlation between topological and chiral properties in full QCD as function of the temperature. On the MILC configurations [37] which use two flavours of staggered quarks we have measured the improved topological charge and the chirality of the lowest eigenvalues of the Dirac operator. Although the renormalization effects on the chirality are large there appears to be a strong correlation between the total chirality carried by the small eigenvalues (unsmoothed) and the total charge of the configuration obtained by IC. Both are also similarly affected by the temperature: above  $T_c$   $Q = 0$  and all Dirac modes become heavy and have vanishing chirality. See Fig. 7 where also the I-A correlation parameter  $c_{\text{int}}$  (6) is drawn.

One even observes local correlation between instantons and Dirac modes [2],[4], the bulks of the corresponding densities seem to overlap quite well.

## 6. Conclusions

The question: which are the vacuum excitations relevant for the dynamics of Yang Mills theories? can be studied in the frame of Euclidean lattice theory by observing the structure of the configurations generated in Monte Carlo simulations. Besides instantons various other proposals have been made, such as super-instantons [38], abelian monopoles or vortices (for recent reviews see, e. g., [39],[40],[41]). We have here been concerned with topological properties, that is with the problem of observing and charac-

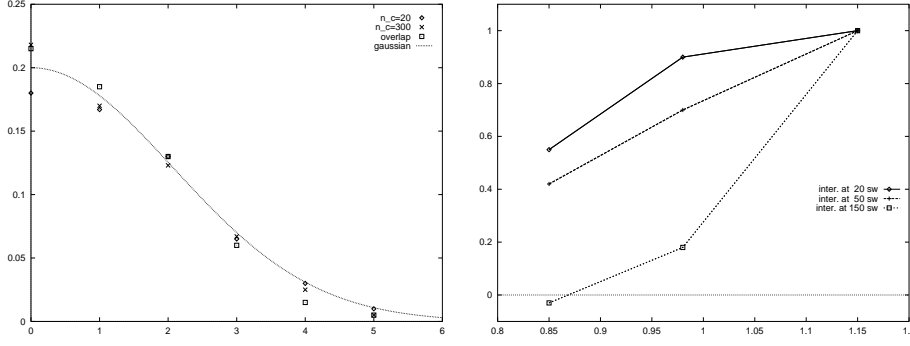


Figure 6. Left: Topological charge distribution for pure  $SU(2)$  by IC at  $n_c = 20$  (diamonds) and  $n_c = 300$  (crosses) and via overlap formalism (squares). The curve is an illustrative Gaussian with arbitrary normalization and slope corresponding to a susceptibility of  $(200 \text{ MeV})^4$ . Right: Temperature dependence of the full QCD data of Fig. 7:  $c_{\text{int}}$  for  $T \sim 0.85, 0.98$  and  $1.13T_c$  after 20 (upper data), 50 (middle) and 150 (lower data) IC cooling sweeps.

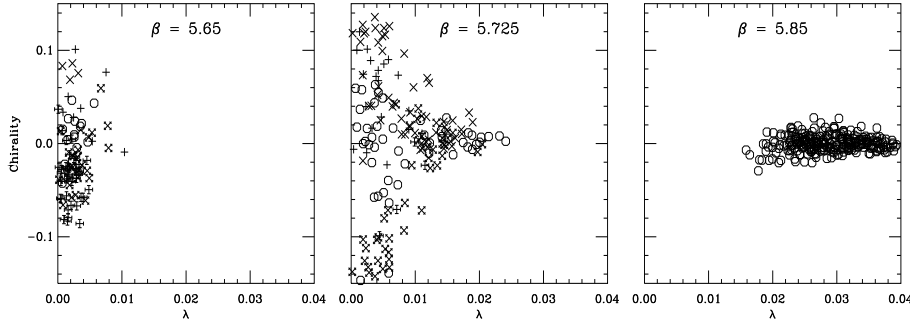


Figure 7. QCD with dynamical quarks: Chirality/eigenvalue plots for the lowest 4 eigenvalues using symbols corresponding to the topological charge for each configuration: octagon ( $Q = 0$ ), cross and fancy cross ( $Q = \pm 1$ ) and plus and fancy plus ( $Q = \pm 2$ ). The three plots correspond to  $T \sim 0.85, 0.98$  and  $1.13T_c$  [7]

terizing the (anti-)instanton ensemble in the MC configurations. Thereby the I's and A's are identified as self-dual structures and fitted to the BPST ansatz. We obtain in this way various results (density, charge and size distributions etc) and we also check the scaling behaviour of these properties under changing of the lattice spacing by factors of the order of 2. In agreement with other studies (see [29],[42] for recent reviews), our results indicate that global observables like the topological susceptibility and charge distributions appear well defined and show good scaling properties. Also some local properties, like size distributions of instantons appear reasonably well defined and scaling. It seems, however, that the topological charge density can fluctuate strongly at small distances and a description

of these fluctuations in terms of instantons and anti-instantons is difficult: the objects do not decrease significantly in size but begin to overlap and become increasingly deformed. While it seems that one can give to some extent “physical” values (by which it is meant: invariant under rescaling of the coupling) for the  $I(A)$  density and overlap if only fluctuations above a given wave-length are retained, these values depend on the latter and it appears difficult to select some “more physical” sub-ensemble characterized by universal parameters.

The connection between topology and chiral properties is well observed at the level of the topological structure which define the topological sector: the instantons which appear responsible for the net topological charge appear also strongly correlated with the Dirac modes of small eigenvalue and large chirality. This connection can also be followed with the temperature.

The analysis of the MC configurations typically needs some procedure to get rid of short range fluctuations. We have used here a “scale controlled cooling algorithm”, RIC, which has been developed to act as a gauge invariant low pass filter. RIC smoothes out fluctuations up to a chosen scale given as a physical (dimensionfull) length and has no other parameter (like setting the number of cooling sweeps  $n_c$  etc). If the smoothing scale is taken large enough this algorithm reproduces standard cooling and it can be used under circumstances to understand the effect of the latter in its dependence on  $n_c$  [43]. Using RIC allows for an independent scaling check, especially in connection with such quantities (like the I-A density) which appear to depend on smoothing, since the smoothing scale is independent on the lattice spacing. In general this smoothing procedure can be used to study the phenomena at a given physical scale and may represent therefore a good instrument in extracting dynamical information from MC configurations.

**Acknowledgments:** Support from the DFG and from the NATO Advanced Research Workshop, Dubna 1999, is thankfully acknowledged.

## References

1. De Forcrand, Ph., García Pérez, M. and Stamatescu, I.-O. (1997), *Nucl. Phys.***B 499**, p. 409, hep-lat/9701012.
2. De Forcrand, Ph., García Pérez, M., Hetrick, J.E. and Stamatescu, I.-O. (1998a) *Nucl. Phys.* [Proc. Suppl.] **63A-C**, p. 549, hep-lat/9710001.
3. De Forcrand, Ph., García Pérez, M., Hetrick, J.E. and Stamatescu, I.-O. (1998b) in *Theory of Elementary particles*, eds. H. Dorn *et al* (Wiley-VCH, Berlin, 1998), p., hep-lat/9802017.
4. De Forcrand, Ph., García Pérez, M., Hetrick, J.E., Laermann, E., Lagae, J.F. and Stamatescu, I.-O. (1999) *Nucl. Phys.* [Proc. Suppl.] **63A-C**, p., hep-lat/9810033.
5. García Pérez, M., Philipsen, O. and Stamatescu, I.-O. (1999a) *Nucl. Phys.***B 551**, p. 293, hep-lat/9812006.
6. García Pérez, M., Philipsen, O. and Stamatescu, I.-O. (1999b) *Nucl. Phys.* [Proc. Suppl.]<sup>4</sup> to appear.

7. De Forcrand *et al* (1999) in *Understanding Deconfinement*, eds. F. Karsch *et al* to appear.
8. Belavin, A.A., Polyakov, A.M., Schwartz, A.A. and Tyupkin, Y.S. (1975) *Phys. Lett.***B59**, p.85.
9. Braam, P.J. and van Baal, P. (1989) *Comm. Math. Phys.* **122**, p.267.
10. Harrington, B.J. and Shepard, H.K. (1978) *Phys. Rev.***D 17** p. 2122.
11. García Pérez, M., González-Arroyo, A., Snippe, J. and van Baal, P. (1994) *Nucl. Phys.***B 413**, p. 535.
12. García Pérez, M., González-Arroyo, A., Montero, A., Pena, C. and van Baal, P. (1999) *JHEP* 9906 001, hep-lat/9903022; *Nucl. Phys.* [Proc. Suppl.]‘ to appear, hep-lat/9909112.
13. Schäfer, T. and Shuryak, E. (1998) *Rev. Mod. Phys.* **70**, p.323.
14. E. Witten (1979) *Nucl. Phys.***B 156**, p.269; G. Veneziano (1979) *Nucl. Phys.***B 159**, p.213.
15. E. Shuryak, *Nucl. Phys.* **B198** (1982) 83.
16. Ilgenfritz, E.-M. and Müller-Preußker, M. (1981) *Nucl. Phys.***B 184**, p. 443; Diakonov, D.I., Petrov, V.Yu. and Pobylyts, P.V. (1989) *Phys. Lett.***B 226**, p. 372.
17. Seiler, E. and Stamatescu, I.-O. (1987) preprint MPI-PAE/PTh 10/87.
18. Pugh, D.J.R. and Teper, M. (1989) *Phys. Lett.***B 224**, p. 159.
19. B. Berg, B. (1981) *Phys. Lett.***B 104**, p. 475; Iwasaki, Y. and T. Yoshie, T. (1983) *Phys. Lett.***B 131**, p. 159; Teper, M. (1985) *Phys. Lett.***B 162**, p. 357; Ilgenfritz, E.M., Laursen, M.L., Schierholz, G., Muller-Preussker, M. and Schiller, A. (1986) *Nucl. Phys.***B 268**, p.693.
20. Feurstein, M., Ilgenfritz, E.M., Müller-Preussker, M. and Thurner, S. (1998) *Nucl. Phys.***B 511**, p. 421; E. M. Ilgenfritz et al. (1998) *Phys. Rev.***D 58**, 094502.
21. T. DeGrand, T., Hasenfratz, A. and Zhu, D. (1996) *Nucl. Phys.***B 475**, p. 321; DeGrand, T., Hasenfratz, A. and Kovacs, T. G. (1997) *Nucl. Phys.***B 505**, p. 417.
22. DeGrand, T., Hasenfratz, A. and Kovacs, T. G. (1998) *Nucl. Phys.***B 520**, p. 301; Hasenfratz, A. and Nietner, C. hep-lat/9810067.
23. Teper, M. (1994) *Nucl. Phys.***B 411**, p. 855; Di Giacomo, A., Meggiolaro, E. and Panagopoulos, H. (1997) *Nucl. Phys.* [Proc. Suppl.] **54A**, p. 343.
24. Campostrini, M., Di Giacomo, A., Maggiore, M., Panagopoulos, H. and Vicari, E. (1989) *Phys. Lett.***B225**, p. 403.
25. De Forcrand, Ph., García Pérez, M. and Stamatescu, I.-O. (1996) ,*Nucl. Phys.* [Proc. Suppl.] **47**, p. 777, hep-lat/9509064.
26. García Pérez and van Baal, P. (1994) *Nucl. Phys.***B 429**, p. 451.
27. Narayanan, R. and Vranas, P. (1997) hep-lat/9702005.
28. Michael, C. and Spencer, P. S. (1995) *Phys. Rev.***D 52**, p. 4691.
29. Negele, J.W. (1999) *Nucl. Phys.* [Proc. Suppl.] , hep-lat/9810053.
30. García Pérez, M., Kovács, T.G. and van Baal, P. (1999) hep-lat/9911485.
31. Smith, D.A. and Teper, M. (1998) *Phys. Rev.***D 58** 014505.
32. Ringwald, A. and Schrempf, F. (1999) *Phys. Lett.***B 459** (1999), p. 249, hep-lat/9903039.
33. Adams, H.D. (2000) hep-lat/0001014.
34. Seiler, E. and Stamatescu, I.-O. (1982) *Phys. Rev.***D 25** 2177; Karsch, F., Seiler, E. and Stamatescu, I.-O. (1986) *Nucl. Phys.***B 271** 349.
35. Alles, B. *et al* (1998) *Phys. Rev.***D 58** 071503
36. Allés, B., D’Elia, M. and Di Giacomo, A. (1997) *Nucl. Phys.***B 494**, p. 281.
37. Bernard, C. *et al* (1996) *Phys. Rev.***D 54**, p. 4585.
38. Patrascioiu, A. and Seiler, E. (1995) *Phys. Rev. Lett.* **75**, p. 2627; hep-lat/9507018.
39. Di Giacomo, A. (1998) *Progr. Theor. Phys. Suppl.* **131**, p 161.
40. Kovacs, T. and Tomboulis, E.T. (1999) hep-lat/9912051.
41. Reinhardt, A. *et al* (1999) hep-th/9911145.
42. Teper, M. (1999) hep-lat/9909124
43. Allés, B., Cosmai, L., D’Elia, M. and Papa, A. (2000) hep-lat/0001027.